Supplementary Information

Enhanced Thermoelectric Properties of Tungsten Disulfide-Multiwalled Carbon Nanotube Composites

Daewoo Suh,‡[a] Dongmok Lee,‡[b] Chanyoung Kang,[c] In-Jin Shon,[d] Woochul Kim[c] and Seunghyun Baik*[b,e,f]

[a] *SKKU Advanced Institute of Nanotechnology (SAINT), Sungkyunkwan University, Suwon, 440-746, Korea*

[b] *Department of Energy Science, Sungkyunkwan University, Suwon, 440-746, Korea*

[c] *School of Mechanical Engineering, Yonsei University, Seoul, 120-749, Korea*

[d] *Division of Advanced Materials Engineering and Research Center of Advanced Materials Development, Engineering College, Chonbuk National University, Jeonbuk, 561-756, Korea*

[e] *Samsung-SKKU Graphene Center, Sungkyunkwan University, Suwon, 440-746, Korea*

[f] *School of Mechanical Engineering, Sungkyunkwan University, Suwon, 440-746, Korea*

* *To whom correspondence should be addressed. E-mail: sbaik@me.skku.ac.kr*

‡ These authors contributed equally to this work.

Experimental section

Sintering of WS_2-MWNT composites: The WS_2-MWNT bulk composites were prepared by powder metallurgy. Firstly, WS_2 (Sigma-Aldrich, 243639, ~99%, 2 μm powder) and thin MWNTs (Hanwha Nanotech, CMP-330F, diameter: 4-7 nm, length: 10-20 μm) were separately dispersed by ultrasonication (ULSSO HI-TECH Co., 560 W, 10 min) in ethanol. The density of thin MWNTs was calculated as 2.34 g cm^{-3} using a previously published protocol [S1]. This is similar with the values reported in literatures [S2-S4]. The suspensions were then combined and further ultrasonicated (560 W, 10 min). The nanotube concentration varied from 0 to 5 wt%. The powder mixture was obtained by filtering the mixture with PTFE membranes (pore size: 0.2 μm) and drying under vacuum (~10^{-2} Torr) for 24 hours at room temperature. In the next step, the dried powder was sintered by a pulsed-current activated combustion system (Eltek) in a vacuum (10^{-1} Torr) [S5]. The T was increased to 1450 °C in ~126 seconds at an applied pressure of 80 MPa as shown in Fig. S2. A pulsed-current (on time: 20 μs, off time: 10 μs) of 2800 A was applied. Finally, the WS_2-MWNT composites were cut (Struers, Minipom) and polished (sand papers) into desired shapes. Disk-shaped specimens (diameter: 12.5 mm, thickness: 0.9-2 mm) were used for thermal conductivity measurements, and rectangular-shaped specimens (2×2×6 mm) were used for electrical conductivity and Seebeck measurements.

Characterization: The electrical conductivity and Seebeck coefficients were measured in a temperature range 300-800 K in helium atmosphere (ULVAC-RIKO, ZEM-3). A Hall effect measurement system (Ecopia, HMS-5000 & AMP-55) based on the van der Pauw method [S6-S8] was used to measure carrier concentration and mobility at room temperature. Four Au-coated oxygen-free bronze probes with a diameter of ~450 μm were employed. The thermal diffusivity (a) was measured by a laser flash method (Netzsch, LFA 457), and the heat capacity (C_p) was obtained by a differential scanning calorimetry method (Netzsch, DSC 200 F3) [S9]. The sample density (ρ) was determined by the sample mass and dimension. The thermal conductivity was determined using the formula, $k = \rho a C_p$ [S10]. SEM (Jeol, JSM-7401F/JSM-7600F) and TEM (Jeol, JEM-3010) images were obtained for powder and sintered specimens. Raman (Kaiser Optical Systems, RXN1, 785nm excitation) spectra were measured for sintered specimens. XRD patterns were obtained for powder (Bruker AXS, D8 FOCUS) and bulk (Bruker AXS, D8 DISCOVER) specimens using Cu k_α radiation (λ = 0.154 nm).

Preparation of WS_2-MWNT composites

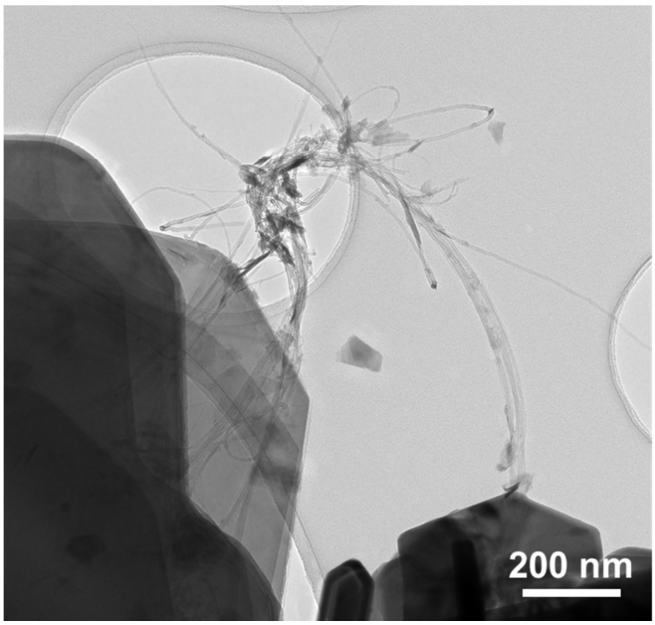

Fig. S1 A TEM image shows the powder mixture of WS_2 and MWNTs.

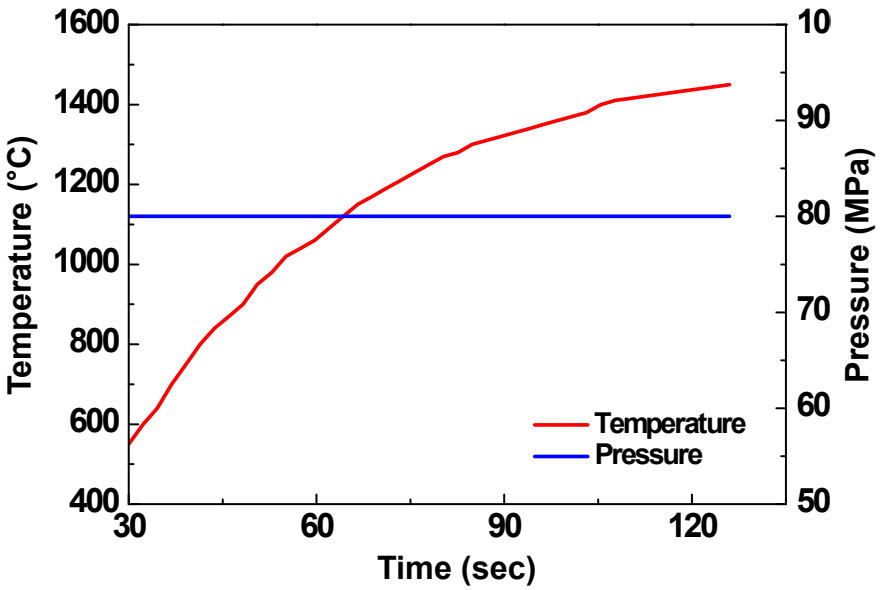

Fig. S2 The temperature and pressure conditions during the sintering process. The sintering was carried out for ~126 seconds, and the pyrometer could record the temperature greater than 550 °C [S5].

Area map of integrated intensity of Raman G-mode of MWNTs

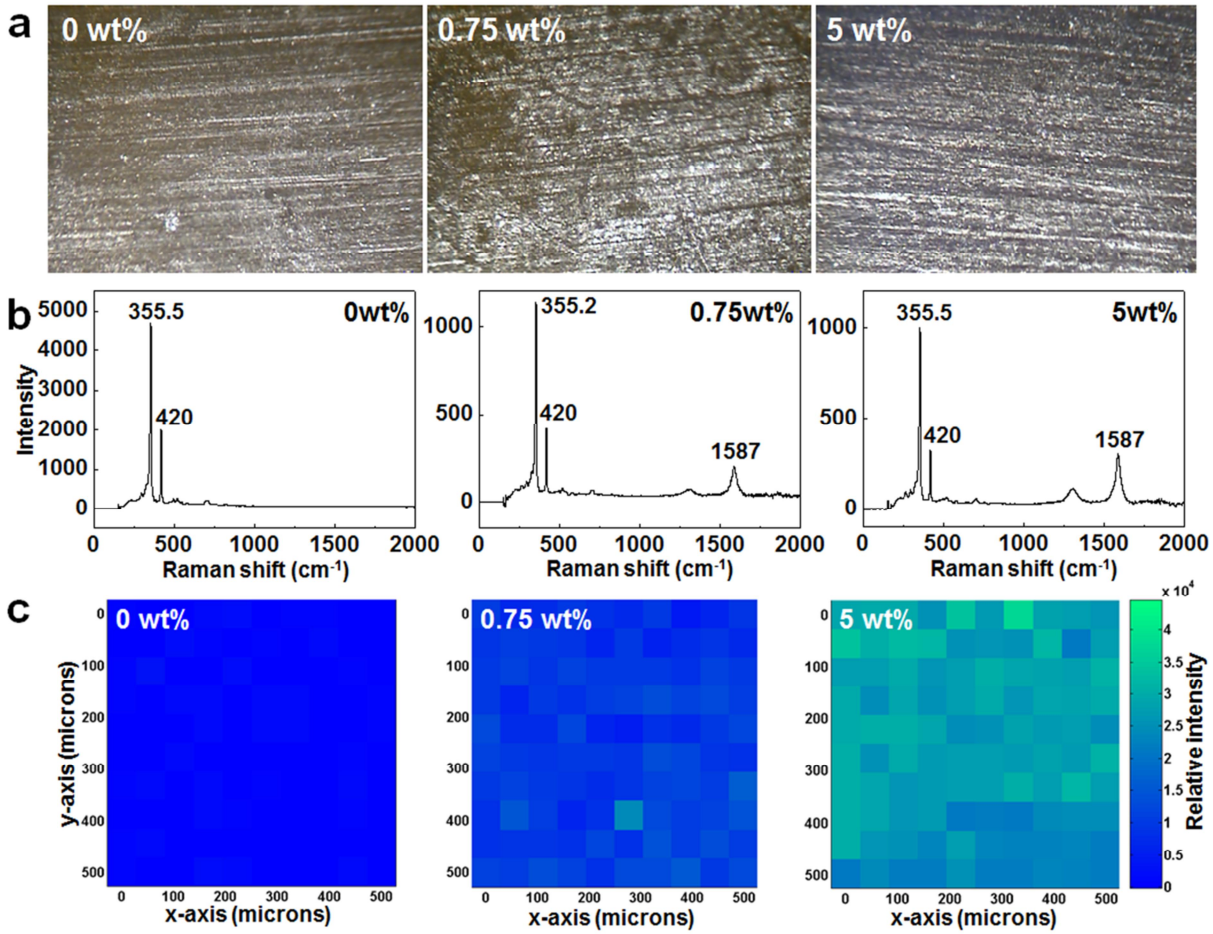

Fig. S3 Area map of integrated intensity of Raman G-mode of nanotubes. Three specimens were investigated (nanotube concentration = 0, 0.75 and 5 wt%). (a) Magnified optical images (10×) of the surface of specimens. (b) The representative Raman spectra of specimens (Kaiser Optical Systems, RXN1, 785nm excitation). The G-mode at ~1587 cm^{-1} is caused by stretching along C-C bonds of carbon nanotubes [S11-S12]. The G-mode intensity increased as the concentration of nanotubes increased. The modes at ~355.5 and 420 cm^{-1} correspond to WS_2 flakes [S13-S14]. (c) Area map of integrated intensity of Raman G-mode of nanotubes. The scanned area was 500×500 μm^2, and the number of pixels was 10×10. The map demonstrates a relatively uniform distribution of carbon nanotubes in the sintered specimen.

XRD analysis of WS_2-MWNT composites

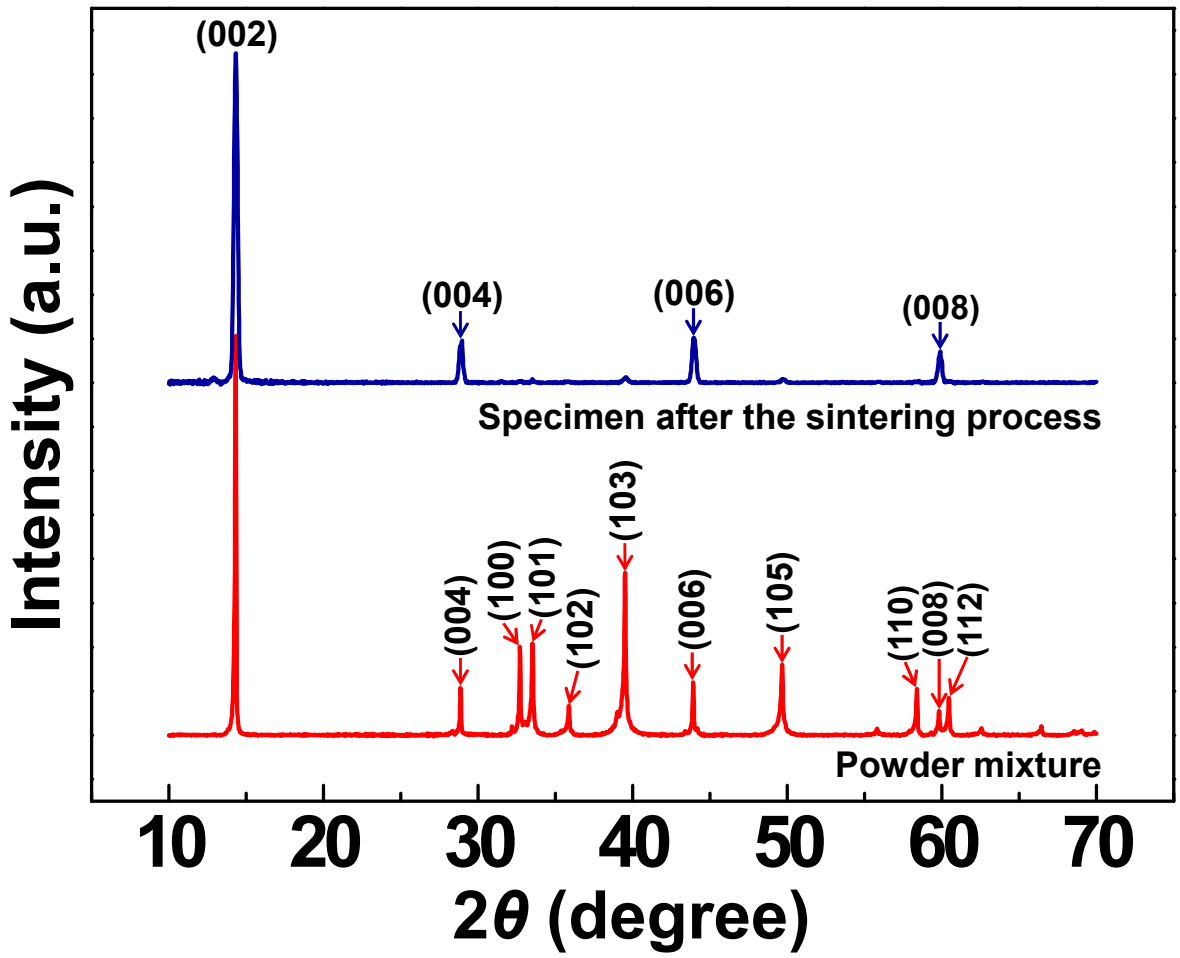

Fig. S4 X-ray diffraction patterns of the powder mixture of WS_2 and MWNTs before and after the sintering process (Powder: Bruker AXS-D8 FOCUS, Bulk Composites: Bruker AXS-D8 DISCOVER, Cu k_α radiation: $\lambda = 0.154$ nm). The nanotube concentration was 0.75 wt%. The peaks related with MWNTs could not be observed clearly probably due to the low concentration. The directions of peaks of WS_2 (JCPDS 08-0237) are denoted.

Microstructures of WS_2-MWNT composites

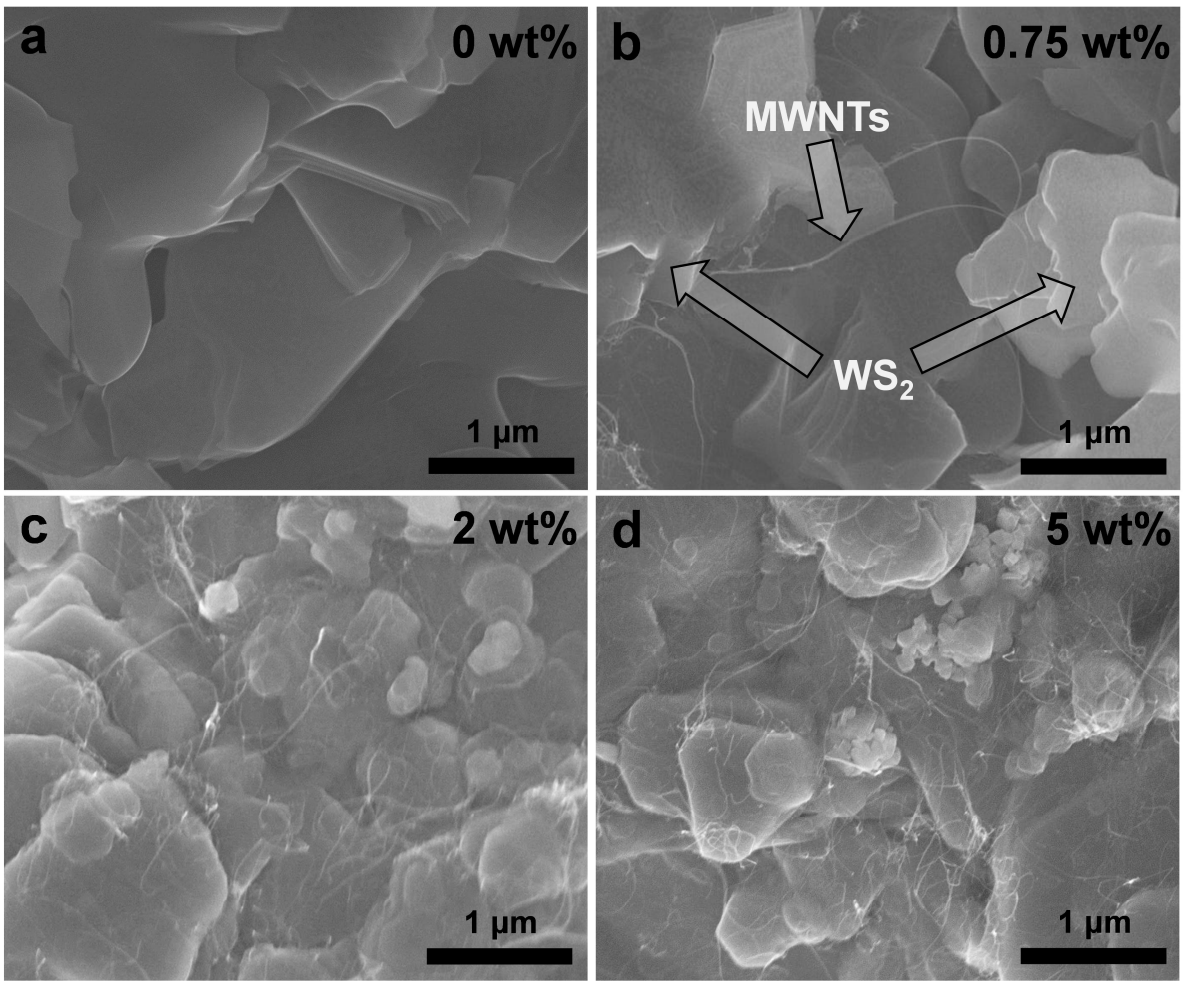

Fig. S5 Cross-sectional SEM images of sintered WS_2-MWNT composites. (a) MWNT concentration = 0 wt% (b) MWNT concentration = 0.75 wt% (c) MWNT concentration = 2 wt% (d) MWNT concentration = 5 wt%.

Physical properties of pure WS_2 and MWNT specimens

The experimentally measured properties of pure WS_2 and MWNT specimens are compared with those in literatures [S15-S21]. There was a reasonable agreement between the data considering the different preparation methods of specimens.

Table S1 Physical properties of pure WS_2 and MWNT specimens.

Material	Sample form	Synthetic method	Carrier concentration [cm^{-3}]	Electrical conductivity [$S\ m^{-1}$]	Reference
WS_2	Thin film	DC magnetron Sputtering	~10^{15}	2.22×10^{-1} ~ 1.00×10^{1}	S15
	Single crystal	Chemical vapor transport technique	1.17×10^{16}	2.63×10^{1}	S16
	Sintered specimen	Sintering [1450 °C, 80 MPa, Pulsed current (2800 A)]	2.28×10^{15}	2.15	Measured in this study
MWNT	Thick film	-	4.00×10^{18}	-	S17
	Aligned film	Vacuum filtration	1.60×10^{19}	~10^{2}	S18
	Sheet sample	Powder pumping [1500 MPa]	3.28×10^{20}	4.00×10^{2} ~ 8.00×10^{2}	S19
	Sintered specimen	Sintering [1700 °C, 50 MPa]	-	6.20×10^{3} ~ 8.30×10^{3}	S20
	Sintered specimen	Sintering [1500 °C, 7 MPa, SPS[a] current (600 A)]	~10^{20}	~10^{4}	S21
	Sintered specimen	Sintering [1450 °C, 80 MPa, Pulsed current (2800 A)]	1.94×10^{19}	4.90×10^{3}	Measured in this study

[a] SPS: spark plasma sintering

Seebeck coefficients of WS_2-MWNT composites

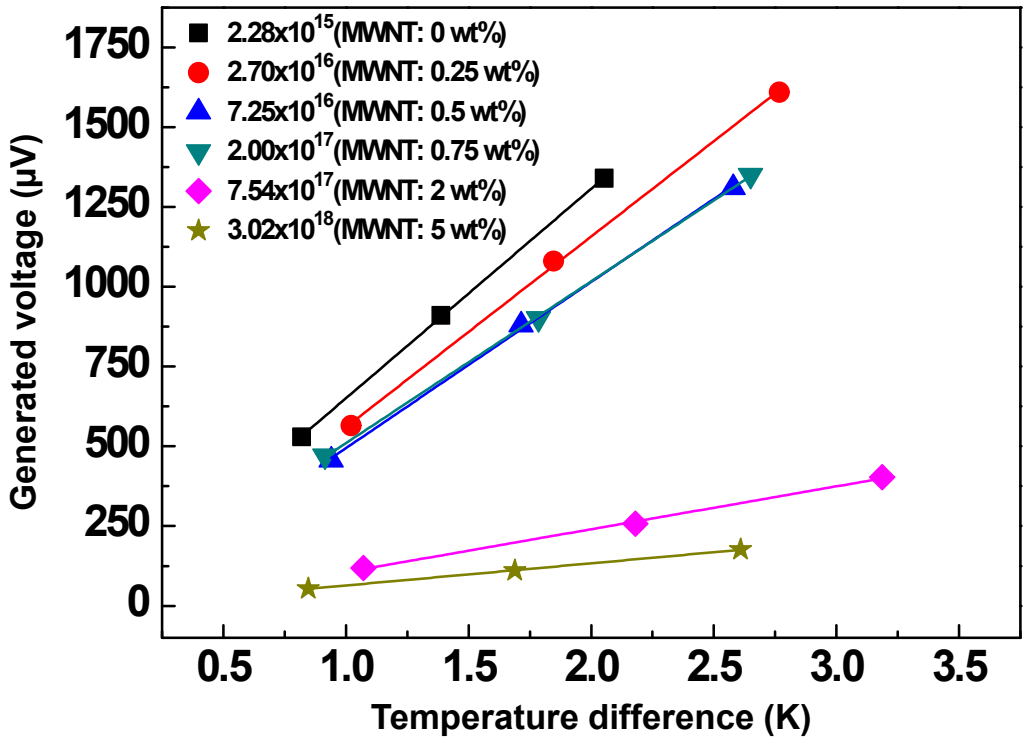

Fig. S6 The thermoelectric voltage is shown as a function of the temperature difference (ULVAC-RIKO, ZEM-3). The measurement was carried out in helium atmosphere at ~300 K. There was a linear relationship between the generated voltage and temperature difference. The carrier concentration and MWNT weight concentration of specimens are shown.

The relative contribution between electronic thermal conductivity and phonon thermal conductivity to the total thermal conductivity

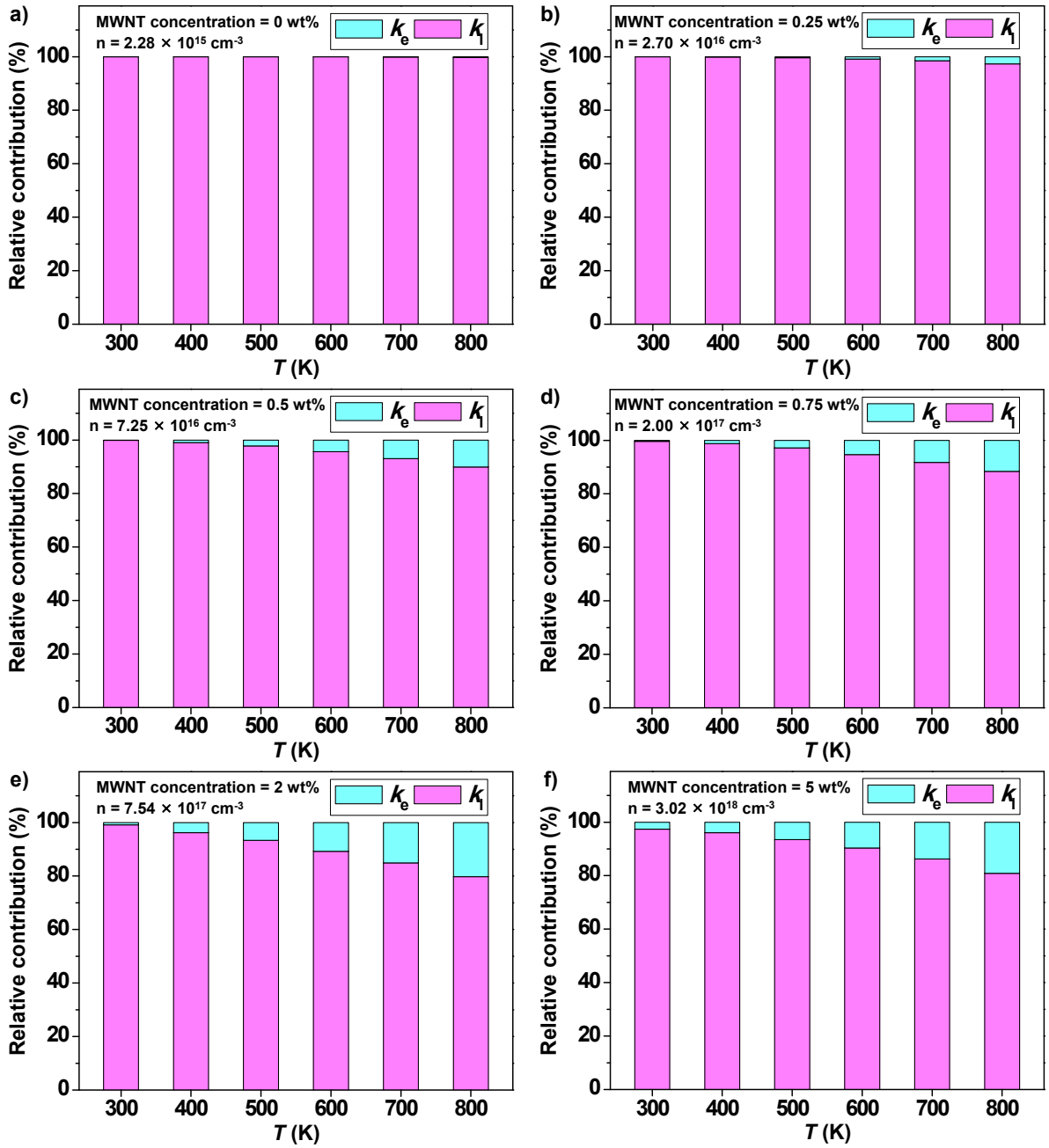

Fig. S7 The relative contribution between electronic thermal conductivity (k_e) and phonon thermal conductivity (k_l) to the total thermal conductivity (k) of WS_2-MWNT composites. (a) MWNT concentration = 0 wt%, $n = 2.28 \times 10^{15}$ cm^{-3} (b) MWNT concentration = 0.25 wt%, $n = 2.70 \times 10^{16}$ cm^{-3} (c) MWNT concentration = 0.5 wt%, $n = 7.25 \times 10^{16}$ cm^{-3} (d) MWNT concentration = 0.75 wt%, $n = 2.00 \times 10^{17}$ cm^{-3} (e) MWNT concentration = 2 wt%, $n = 7.54 \times 10^{17}$ cm^{-3} (f) MWNT concentration = 5 wt%, $n = 3.02 \times 10^{18}$ cm^{-3}.

References

[S1] Ch. Laurent, E. Flahaut and A. Peigney, *Carbon*, 2010, **48**, 2994.

[S2] G. Chen, H. Kim, B. H. Park and J. Yoon, *Polymer*, 2006, **47**, 4760.

[S3] T. A. Saleh and V. K. Gupta, *J. Colloid Interface Sci.*, 2011, **362**, 337.

[S4] W. Yuan, J. Che and M. B. Chan-Park, *Chem. Mat.*, 2011, **23**, 4149.

[S5] I. Shon, J. Park, I. Ko, J. Doh, J. Yoon and K. Nam, *Ceram. Int.*, 2011, **37**, 1549.

[S6] T. M. Tritt, in *Thermoelectrics handbook: macro to nano*, ed. D. M. Rowe, CRC press, Boca Raton, 2006, ch. 23.

[S7] S. Jeon, M. Oh, H. Jeon, S. D. Kang, H. Lyeo, S. Hyun and H. Lee, *J. Electrochem. Soc.*, 2011, **158**, H808.

[S8] S. Hong, E. Kim, W. Kim, S. Jeon, S. C. Lim, K. Kim, H. Lee, S. Hyun, D. Kim, J. Choi, Y. H. Lee and S. Baik, *Phys. Chem. Chem. Phys.*, 2012, DOI: 10.1039/C2CP42936E.

[S9] Y. Choi, Y. Kim, S. Park, Y. Kim, B. J. Sung, S. Jang and W. Kim, *Org. Electron.*, 2011, **12**, 2120.

[S10] F. P. Incropera, D. P. Dewitt, T. L. Bergman and A. S. Lavine, in *Fundamentals of Heat and Mass Transfer*, ed. F. P. Incropera, D. P. Dewitt, T. L. Bergman and A. S. Lavine, John Wiley & Sons, 6th edn., Asian Student edn., 2007, ch. 2, p. 68.

[S11] D. A. Heller, S. Baik, T. E. Eurell and M. S. Strano, *Adv. Mater.*, 2005, **17**, 2793.

[S12] R. Saito, G. Dresselhaus and M. S. Dresselhaus, in *Physical Properties of Carbon Nanotubes*, ed. R. Saito, G. Dresselhaus and M. S. Dresselhaus, Imperial College Press, London, 1998.

[S13] T. Sekine, T. Nakashizu, K. Toyoda, K. Uchinokura and E. Matsuura, *Solid State Commun.*, 1980, **35**, 371.

[S14] M. Krause, M. Viršek, M. Remškar, N. Salacan, N. Fleischer, L. Chen, P. Hatto, A. Kolitsch and W. Möller, *ChemPhysChem*, 2009, **10**, 2221.

[S15] K. Ellmer, C. Stock, K. Diesner and I. Sieber, *J. Cryst. Growth*, 1997, **182**, 389.

[S16] G. K. Solanki, D. N. Gujarathi, M. P. Deshpande, D. Lakshminarayana and M. K. Agarwal, *Cryst. Res. Technol.*, 2008, **43**, 179.

[S17] L. Forró and C. Schönenberger, in *Carbon nanotubes: synthesis, structure, properties, and applications*, ed. M. S. Dresselhaus, G. Dresselhaus and P. Avouris, Springer, Berlin, 2001, p. 369.

[S18] G. Baumgartner, M. Carrard, L. Zuppiroli, W. Bacsa, W. D. Heer and L. Forró, *Phys. Rev. B*, 1997, **55**, 6704.

[S19] P. C. Ma, B. Z. Tang and J. Kim, *Chem. Phys. Lett.*, 2008, **458**, 166.

[S20] C. Qin, X. Shi, S. Q. Bai, L. D. Chen and L. J. Wang, *Mater. Sci. Eng. A-Struct. Mater. Prop. Microstruct. Process.*, 2006, **420**, 208.

[S21] K. Yang, J. He, Z. Su, J. B. Reppert, M. J. Skove, T. M. Tritt and A. M. Rao, *Carbon*, 2010, **48**, 756.